Electronic Supplementary Material (ESI) for Journal of Materials Chemistry A.

Supporting Information

Dye Sensitized Solar Cells with Cobalt and Iodine-Based Electrolyte: The Role of Thiocyanate-Free Ruthenium Sensitizers

Kuan-Lin Wu,[a,‡] Yue Hu,[b,‡] Chun-Tien Chao,[a] Ya-Wen Yang,[a] Ting-Yun Hsiao,[c] Neil Robertson,*[,b] and Yun Chi,*[,a]

[a] Department of Chemistry and Low Carbon Energy Research Center, National Tsing Hua University, Hsinchu 30013, Taiwan; E-mail: ychi@mx.nthu.edu.tw

[b] EaStCHEM, School of Chemistry, University of Edinburgh, King's Buildings, West Mains Road, Edinburgh EH9 3 JJ (UK); E-mail: Neil.Robertson@ed.ac.uk

[c] Department of Engineering and System Science, National Tsing Hua University, Hsinchu 30013, Taiwan

‡ K-L W and Y H contributed equally to this work.

Computational Methodology:

The molecular structures were optimised in vacuum, using the software Avogadro [1] to enter the starting geometry. Then the structure was optimised in dimethylformamide (DMF), using the optimised structure from vacuum. All calculations were carried out using the Gaussian 09 program [2] with the Becke three parameter exchange functional with the Perdew Wang 1991 correlation functional (B3PW91) [3] level of theory together with 6-31+G basis set for C, H, N, O, F and S atoms. The Ru atom was treated with the Hay-Wadt VDZ (n+1) ECP basis set. [4] Time-dependent DFT calculations (TD-DFT) [5] were performed using the Gaussian 09 program with a polarisable continuum model (PCM) in DMF. [6] The 70 lowest singlet electronic transitions were calculated and processed with the GaussSum software package. [7]

Calculation of hole diffusion coefficents was carried out using the following equation:

$$D_{app}=5.02k_BTj_p^2/q^3c_0^2v$$

k_B Boltzmann constant 1.38*10^{-23}(JK^{-1})

T temperature 295(K)

j_p peak current density of the cyclic volammogram (Acm^{-2})

q electron elementary charge 1.602*10^{-19} (C)

c_0 dye loading expressed as volume concentration (cm^{-3})

v scan rate $1Vs^{-1}$

The volume concentration of dye molecules (C_0) attached to the TiO_2 mesoporous films upon sensitization was determined via UV-vis spectroscopy. The dye desorption experiment was performed using 1M NaOH in water/EtOH(v/v, 1:1).

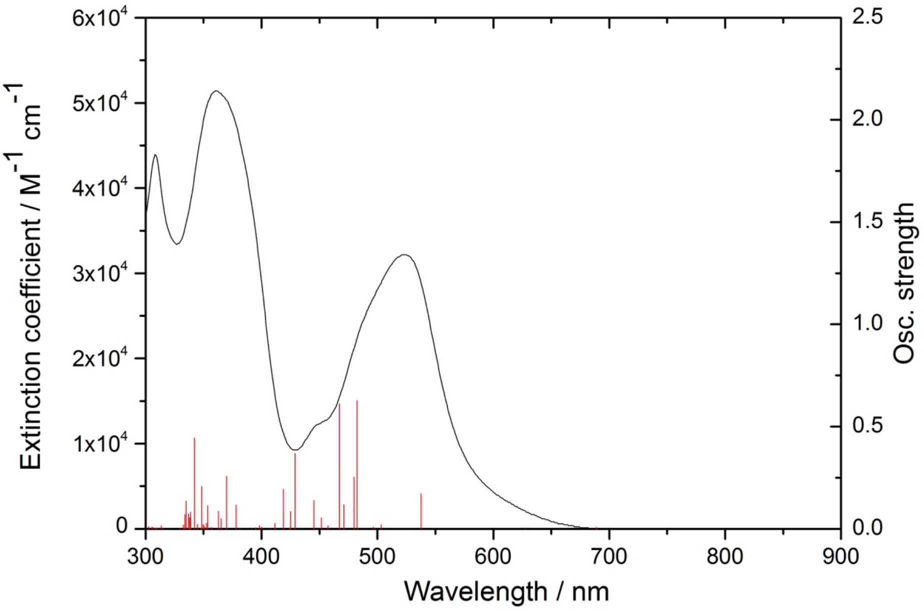

Figure S1. Experimental UV-visible spectra (black line) and computational simulated Oscillator strength (red line) of TFRS-80a.

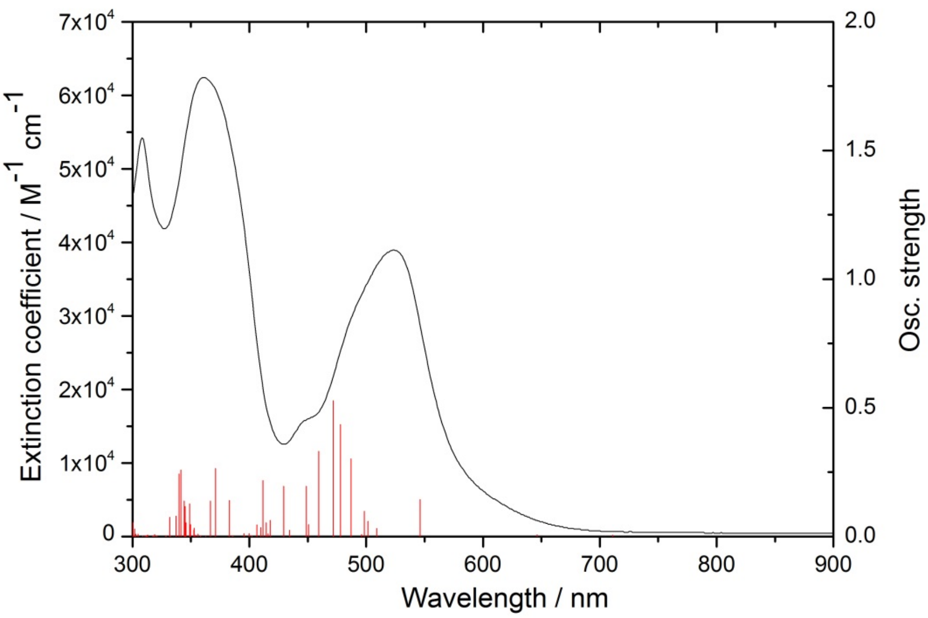

Figure S2. Experimental UV-visible spectra (black line) and computational simulated Oscillator strength (red line) of TFRS-80b.

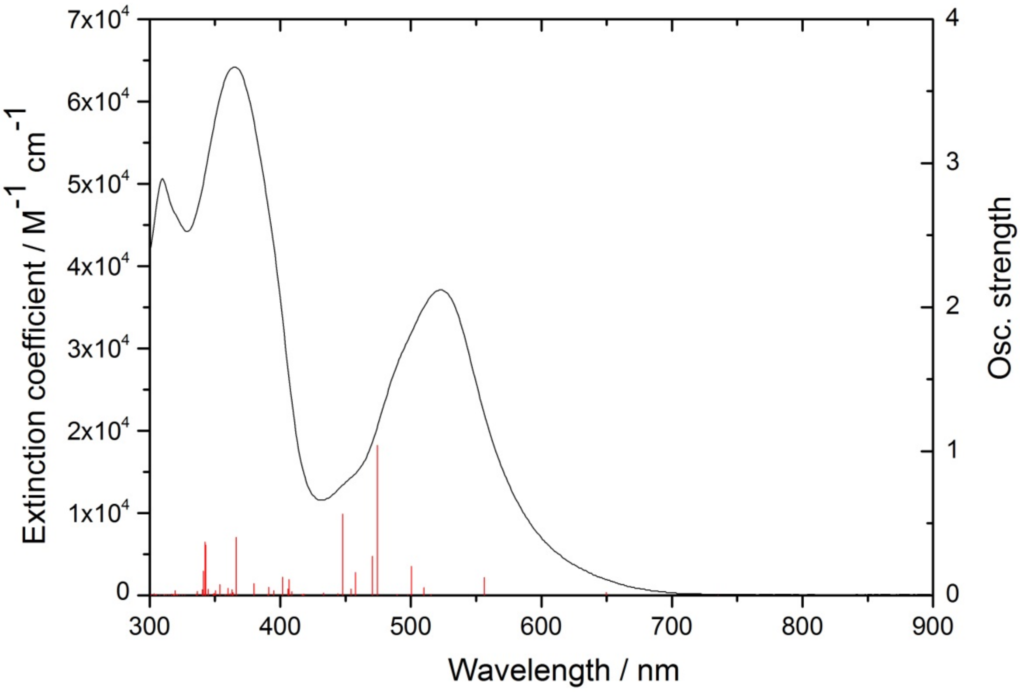

Figure S3. Experimental UV-visible spectra (black line) and computational simulated Oscillator strength (red line) of TFRS-80c.

TFRS-80a

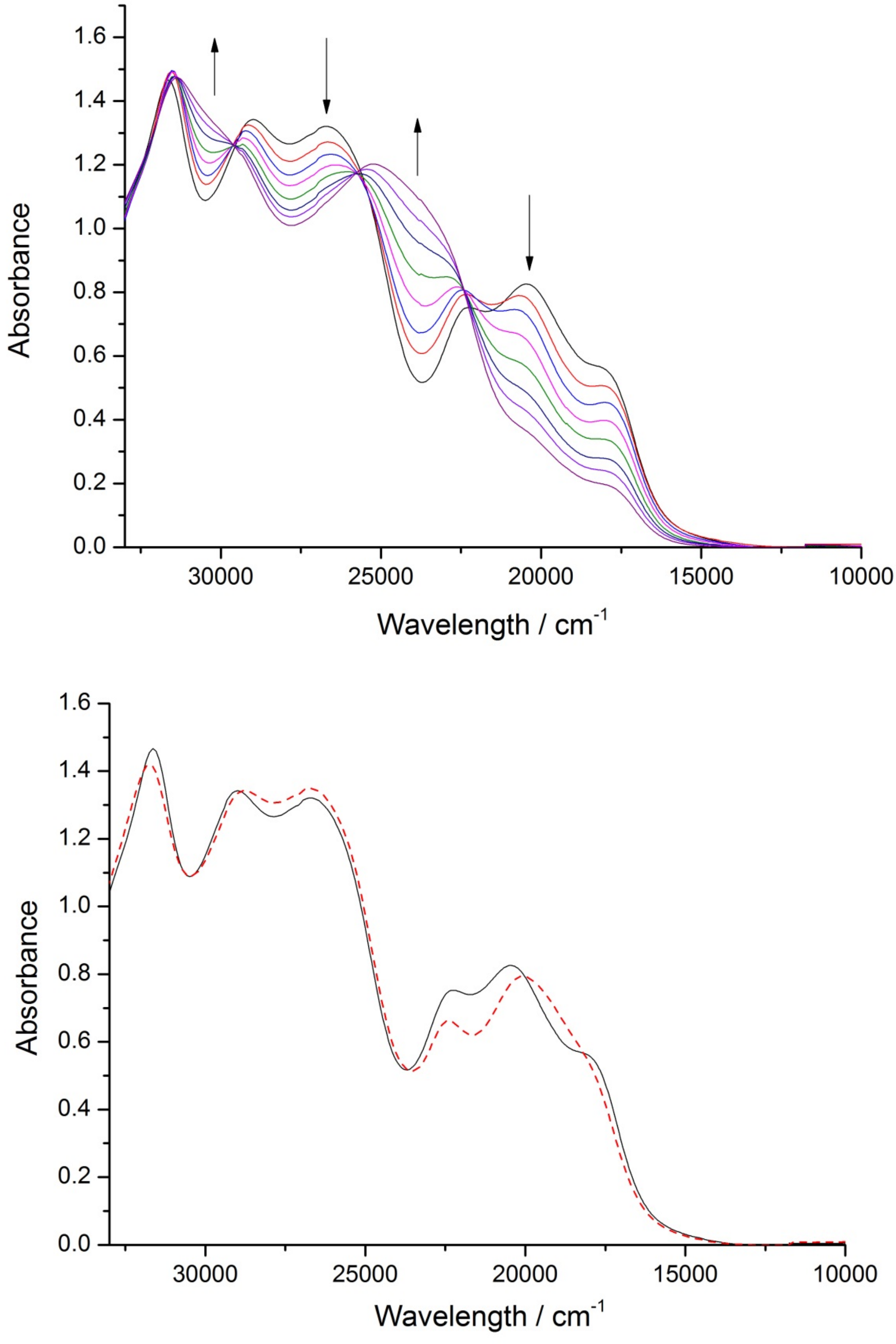

Figure S4. (a) Oxidative spectroelectrochemical studies of **TFRS-80a** in 0.1 M $TBABF_6$/DMF with an applied potential of +1.1 V (vs. Ag/AgCl). (b) overlay of initial and final spectra to show that regeneration of **TFRS-80a** did not fully occur. The studies were carried out at -8 ^{o}C. The regeneration process was carried out at +0.27 V.

TFRS-80b

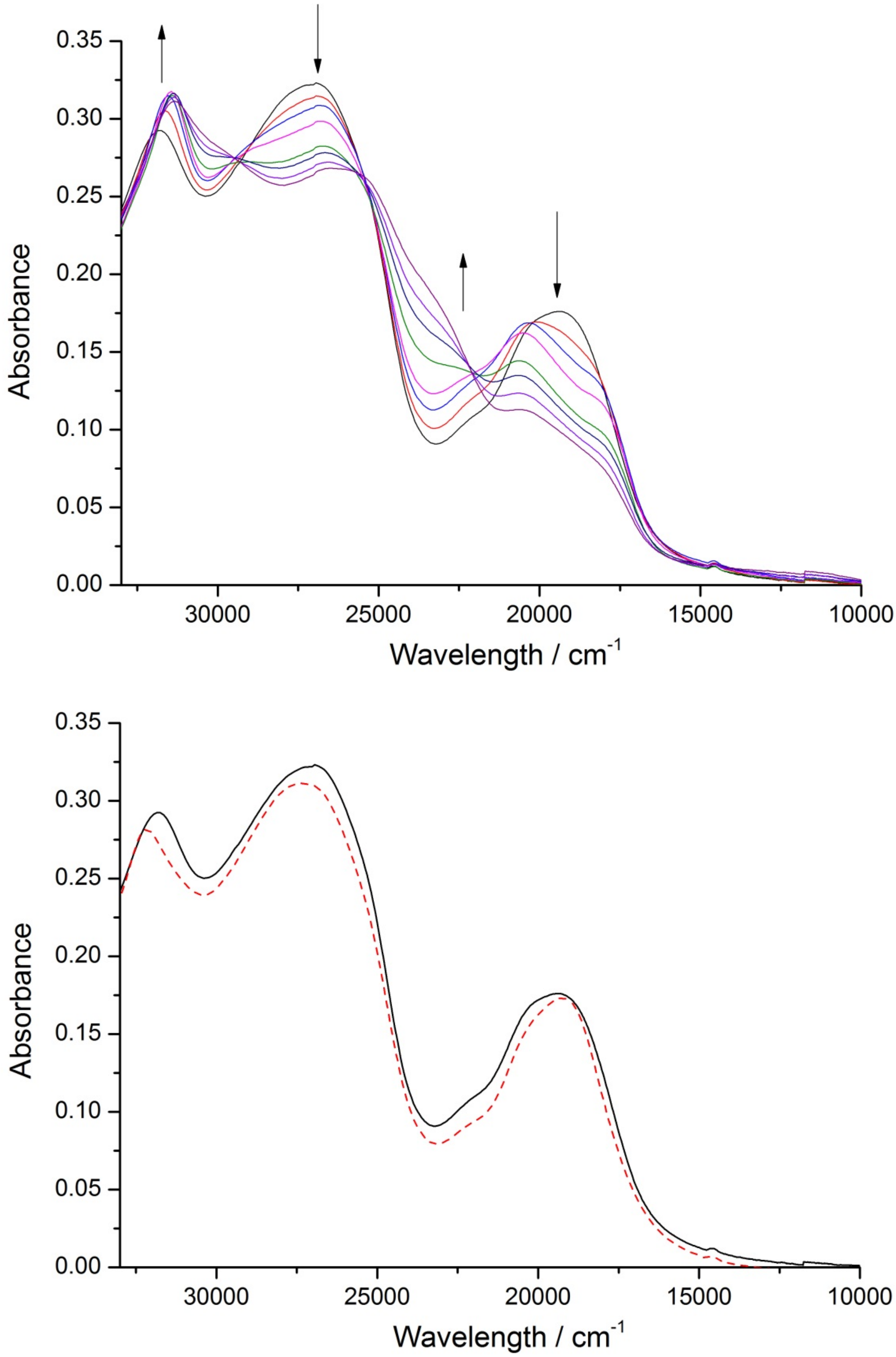

Figure S5. Oxidative spectroelectrochemistry studies of **TFRS-80b** in 0.1 M $TBABF_6$/DMF with an applied potential of +1.1 V (vs. Ag/AgCl). (b) overlay of initial and final spectra to show regeneration of **TFRS-80b** occurred. The studies were carried out at -8°C. The regeneration process was carried out at +0.18 V.

TFRS-80c

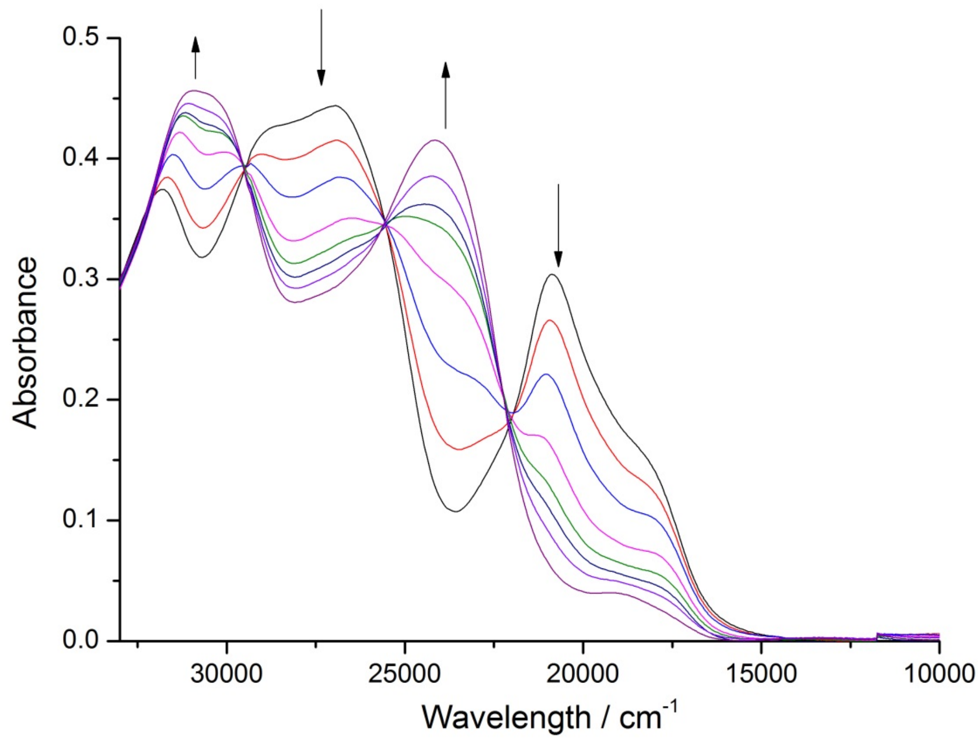

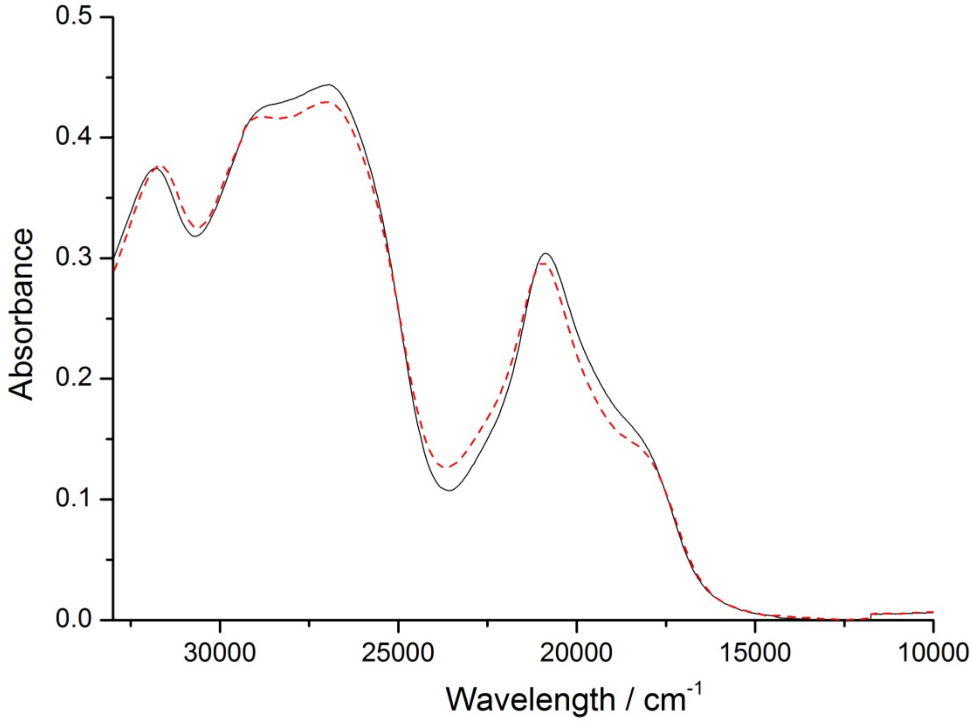

Figure 6S. Oxidative OTTLE studies of **TFRS-80c** in 0.1 M $TBABF_6$/DMF with an applied potential of +1 V (vs. Ag/AgCl). (b) overlay of initial and final spectra to show regeneration of **TFRS-80c** occurred. The studies were carried out at -12^{o}C. The regeneration process was carried out at +0.31 V.

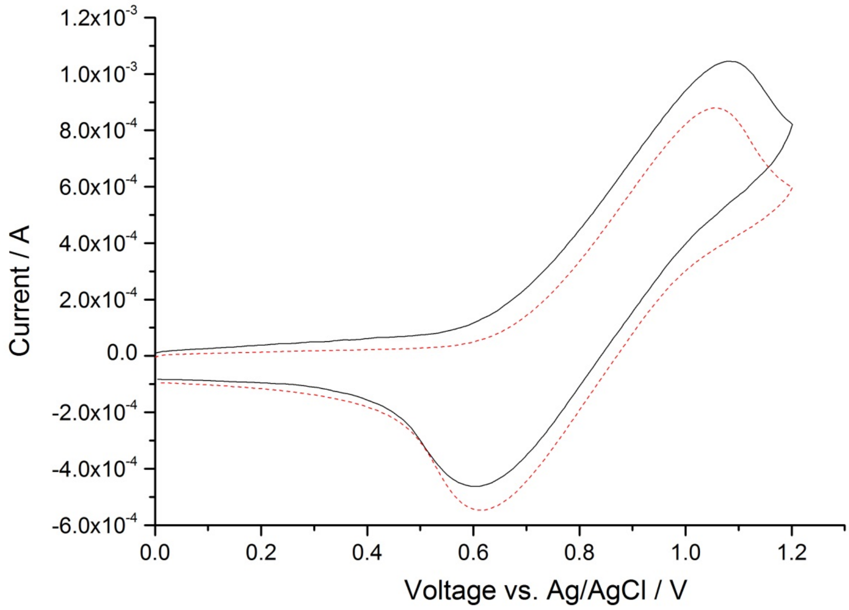

Fig. S7 Cyclic volatammogram of TFRS-80a attached to TiO_2 nanocrystalline films showing the first cycle (black solid line) and the 51^{st} cycle (red dashed line) at scan rate 1 V/s.

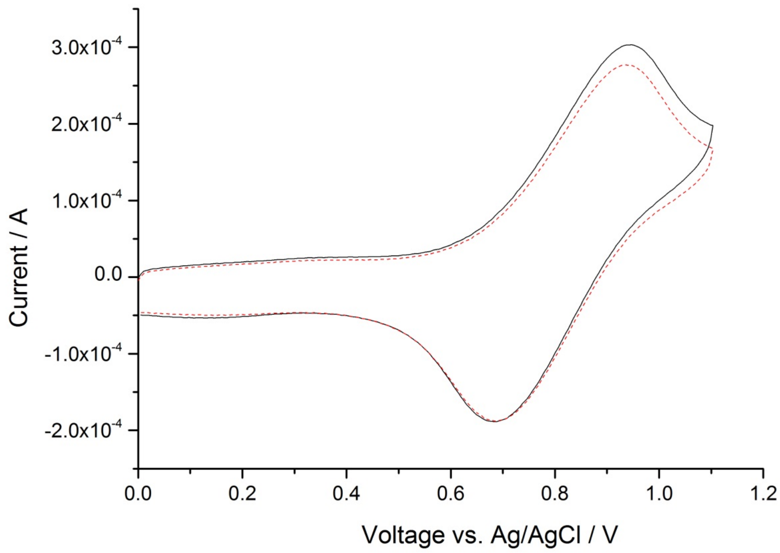

Figure S8 Cyclic volatammogram of TFRS-80b attached to TiO_2 nanocrystalline films showing the first cycle (black solid line) and the 51^{st} cycle (red dashed line) at scan rate 1 V/s.

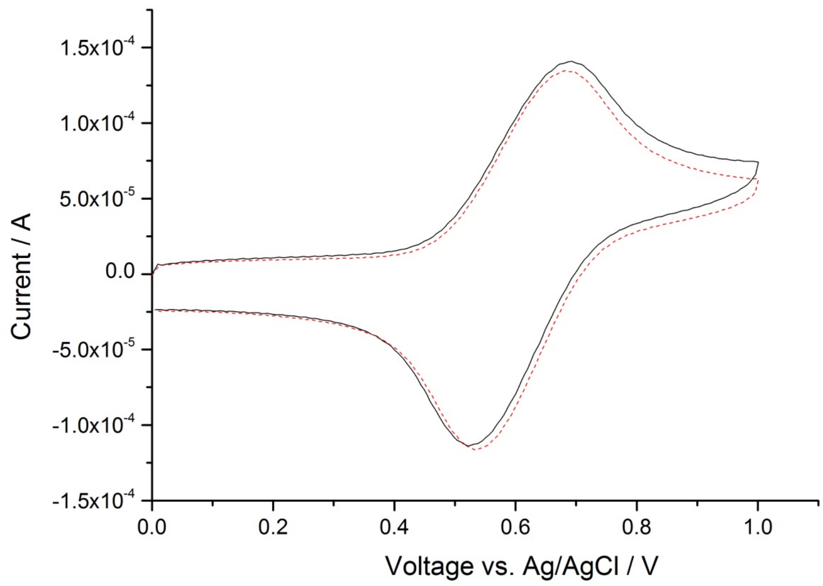

Figure S9 Cyclic volatammogram of TFRS-80c attached to TiO_2 nanocrystalline films showing the first cycle (black solid line) and the 51^{st} cycle (red dashed line) at scan rate 1 V/s.

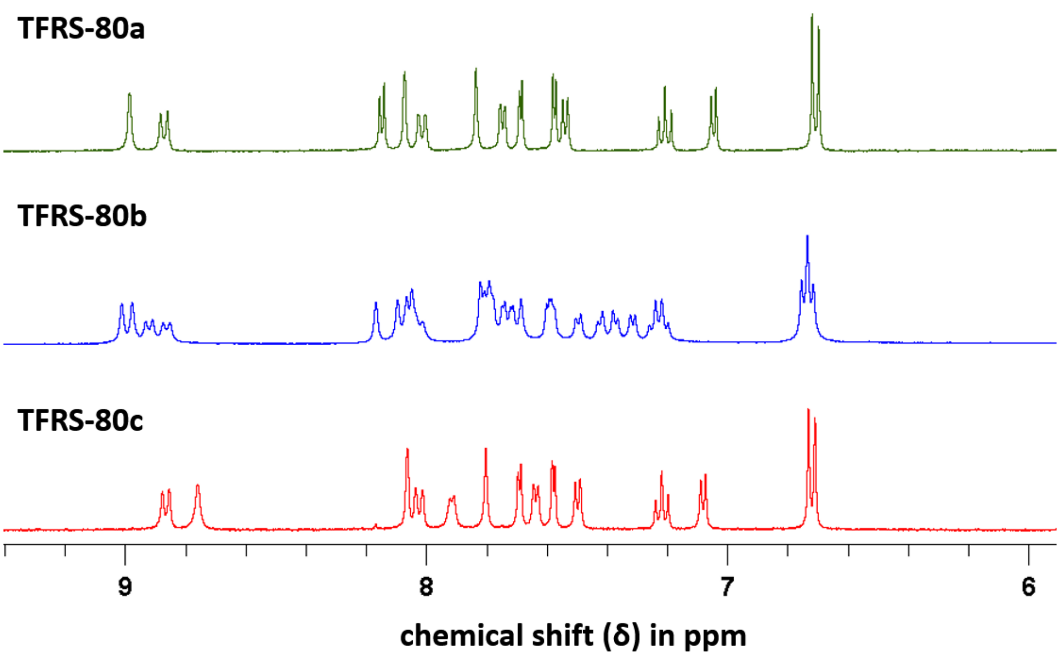

Figure S10. ^{1}H NMR of isomeric sensitizers TFRS-80a, b and c in the downfield region of aromatic protons.

Table S1. The wavelengths, oscillator strengths and major contributions of the singlet optical transitions in selected states with oscillator strength > 0.1 for TFRS-80a dye in DMF.

No.	Wavelength (nm)	Osc. Strength	Major contribs
1	688.94	0.0089	H-1 → LUMO (73%), HOMO → LUMO (23%)
3	537.66	0.1713	H-3 → LUMO (70%), H-1 → L+2 (16%)
7	482.39	0.627	H-1 → L+1 (24%), HOMO → L+1 (51%)
8	479.70	0.2521	H-1 → L+2 (11%), HOMO → L+2 (46%), HOMO → L+3 (20%)
9	470.99	0.1179	H-4 → LUMO (57%), HOMO → LUMO (20%), HOMO → L+1 (12%)
10	467.23	0.6109	H-1 → L+2 (41%), HOMO → L+2 (29%), HOMO → L+3 (10%)
13	445.21	0.1384	H-3 → L+2 (67%), H-3 → L+3 (20%)
14	428.92	0.3687	H-2 → L+1 (78%)
17	418.89	0.1949	H-2 → L+2 (35%), H-2 → L+3 (44%)
27	378.03	0.1164	H-4 → L+3 (64%)
28	369.74	0.2579	HOMO → L+5 (72%)
32	353.46	0.1137	H-7 → L+1 (44%), H-1 → L+6 (29%)
36	348.37	0.2077	H-7 → L+1 (24%), H-1 → L+6 (53%)
39	342.27	0.4438	H-8 → L+1 (51%), H-7 → L+3 (18%)
43	334.91	0.1359	H-8 → L+3 (70%), HOMO → L+6 (14%)

Table S2. The wavelengths, oscillator strengths and major contributions of the singlet optical transitions in selected states with oscillator strength > 0.1 for TFRS-80b dye in DMF.

No.	Wavelength (nm)	Osc. Strength	Major contribs
1	710.9544	0.0058	H-2 → LUMO (20%), H-1 → LUMO (15%), HOMO → LUMO (56%)
2	646.3188	0.0071	H-3 → LUMO (20%), H-1 → LUMO (44%),
3	546.158	0.1441	H-4 → LUMO (11%), H-3 → LUMO (10%), H-2 → LUMO (44%), H-1 → LUMO (15%)
8	486.9922	0.3018	H-4 → LUMO (26%), H-1 → LUMO (11%), H-1 → L+1 (22%), HOMO → L+1 (15%)
9	477.9067	0.4357	H-4 → LUMO (17%), H-1 → L+2 (28%), HOMO → L+2 (16%)
10	471.8142	0.5279	H-4 → LUMO (12%), H-1 → L+1 (24%), H-1 → L+2 (13%), HOMO → L+3 (14%)
11	459.5209	0.331	H-2 → L+1 (23%), H-2 → L+3 (16%), H-1 → L+1 (15%)
13	448.7435	0.1952	H-2 → L+1 (18%), H-2 → L+3 (30%)
15	429.439	0.1952	H-7 → LUMO (19%), H-1 → L+3 (21%)
19	411.727	0.218	H-3 → L+2 (30%), H-3 → L+3 (16%)
27	383.0784	0.1407	H-4 → L+2 (15%), H-4 → L+3 (31%),
28	371.0743	0.2646	HOMO → L+5 (49%), HOMO → L+6 (23%)
29	366.6519	0.1377	H-1 → L+5 (28%), H-1 → L+6 (27%)
37	348.7576	0.127	H-7 → L+2 (59%), H-5 → L+3 (11%)
39	344.9059	0.1173	H-2 → L+6 (26%),H-1 → L+6 (15%)
40	344.2547	0.1376	H-8 → L+2 (20%), H-7 → L+3 (50%),
41	341.4484	0.2581	H-8 → L+2 (57%), H-8 → L+3 (11%)
42	339.9318	0.2436	H-8 → L+3 (72%)

Table S3. The wavelengths, oscillator strengths and major contributions of the singlet optical transitions in selected states with oscillator strength > 0.1 for TFRS-80c dye in DMF.

No.	Wavelength (nm)	Osc. Strength	Major contribs
1	735.54	0.0018	H-1 → LUMO (94%)
3	556.35	0.1241	H-4 → LUMO (13%), H-2 → LUMO (72%)
5	510.01	0.0538	H-1 → L+2 (89%)
6	500.42	0.2012	H-3 → LUMO (56%), HOMO → LUMO (34%)
9	474.29	1.0422	H-3 → L+2 (11%), HOMO → L+2 (70%)
10	470.58	0.2712	H-4 → LUMO (16%), HOMO → L+1 (56%)
11	457.52	0.1596	H-4 → L+1 (16%), H-2 → L+1 (72%)
13	447.75	0.5637	H-4 → L+3 (17%), H-2 → L+3 (65%)
20	406.60	0.1094	H-4 → L+1 (40%), H-3 → L+2 (14%),
22	401.70	0.1248	H-4 → L+1 (18%), H-3 → L+2 (53%),
24	391.13	0.0548	H-4 → L+3 (47%), H-2 → L+3 (22%)
27	379.73	0.081	H-4 → L+2 (10%), H-3 → L+3 (41%)
28	366.26	0.4022	H-3 → L+4 (15%), HOMO → L+5 (34%)
34	353.89	0.0744	H-7 → L+1 (84%)
39	342.93	0.3485	H-8 → L+2 (16%), H-7 → L+3 (24%), HOMO → L+6 (35%)
40	342.54	0.3688	H-8 → L+2 (27%), H-2 → L+5 (49%)
41	341.06	0.1686	H-7 → L+2 (13%), H-2 → L+6 (41%)

Table S4: Peak current densities, adsorbed concentrations and hole diffusion coefficients for the isomers

	j_p / Acm^{-2}	$c_0 \times 10^{19}$/ cm^{-3}	D_{app} / $cm^2\ s^{-1}$
TFRS-80a	1.04×10^{-3}	11.3	4.21×10^{-10}
TFRS-80b	3.03×10^{-4}	5.96	1.28×10^{-10}
TFRS-80c	1.41×10^{-4}	6.98	2.03×10^{-11}

[1] M. D. Hanwell *et al*. *J. Cheminfor*. **2012**, *4*, 17.
[2] Gaussian 09, Revision A.02, M. J. Frisch, G. W. Trucks, H. B. Schlegel, G. E. Scuseria, M. A. Robb, J. R. Cheeseman, G. Scalmani, V. Barone, B. Mennucci, G. A. Petersson, H. Nakatsuji, M. Caricato, X. Li, H. P. Hratchian, A. F. Izmaylov, J. Bloino, G. Zheng, J. L. Sonnenberg, M. Hada, M. Ehara, K. Toyota, R. Fukuda, J. Hasegawa, M. Ishida, T. Nakajima, Y. Honda, O. Kitao, H. Nakai, T. Vreven, J. A. Montgomery, Jr., J. E. Peralta, F. Ogliaro, M. Bearpark, J. J. Heyd, E. Brothers, K. N. Kudin, V. N. Staroverov, R. Kobayashi, J. Normand, K. Raghavachari, A. Rendell, J. C. Burant, S. S. Iyengar, J. Tomasi, M. Cossi, N. Rega, J. M. Millam, M. Klene, J. E. Knox, J. B. Cross, V. Bakken, C. Adamo, J. Jaramillo, R. Gomperts, R. E. Stratmann, O. Yazyev, A. J. Austin, R. Cammi, C. Pomelli, J. W. Ochterski, R. L. Martin, K. Morokuma, V. G. Zakrzewski, G. A. Voth, P. Salvador, J. J. Dannenberg, S. Dapprich, A. D. Daniels, O. Farkas, J. B. Foresman, J. V. Ortiz, J. Cioslowski, and D. J. Fox, Gaussian, Inc., Wallingford CT, 2009.
[3] (a) Perdew, J. P.; Chevary, J. A.; Vosko, S. H.; Jackson, K. A.; Pederson, M. R.; Singh, D. J.; Fiolhais, C., Atoms, Molecules, Solids, and Surfaces - Applications of the Generalized Gradient Approximation for Exchange and Correlation (Vol 46, Pg 6671, 1992). *Phys Rev B* **1993,** *48* (7), 4978-4978; (b) Perdew, J. P.; Burke, K.; Wang, Y., Generalized gradient approximation for the exchange-correlation hole of a many-electron system. *Phys Rev B* **1996,** *54* (23), 16533-16539.
[4] (a) Hay, P. J.; Wadt, W. R., Abinitio Effective Core Potentials for Molecular Calculations - Potentials for K to Au Including the Outermost Core Orbitals. *J Chem Phys* **1985,** *82* (1), 299-310; (b) Hay, P. J.; Wadt, W. R., Abinitio Effective Core Potentials for Molecular Calculations - Potentials for the Transition-Metal Atoms Sc to Hg. *J Chem Phys* **1985,** *82* (1), 270-283; (c) Wadt, W. R.; Hay, P. J., Abinitio Effective Core Potentials for Molecular Calculations - Potentials for Main Group Elements Na to Bi. *J Chem Phys* **1985,** *82* (1), 284-298.
[5] (a) Bauernschmitt, R. Ahlrichs, *Chem Phys Lett* **1996**, *256*, 454-464; (b) D. J. Tozer, N. C. Handy, *J Chem Phys* **1998**, *109*, 10180-10189.
[6] Cossi, M.; Barone, V. J. Chem. Phys. 2001, 115, 4708–4717.
[7] O'Boyle, N. M.; Tenderholt, A. L.; Langner, K. M. J. Comput. Chem. 2008, 29 (5), 839-845.